

# Design of Organic Structures in the Solid State: Molecular Tapes Based on the Network of Hydrogen Bonds Present in the Cyanuric Acid-Melamine Complex

Jonathan A. Zerkowski, John C. MacDonald, Christopher T. Seto, Derk A. Wierda, and George M. Whitesides\*

Contribution from the Department of Chemistry, Harvard University,  
 Cambridge, Massachusetts 02138

Received August 11, 1992. Revised Manuscript Received January 10, 1994®

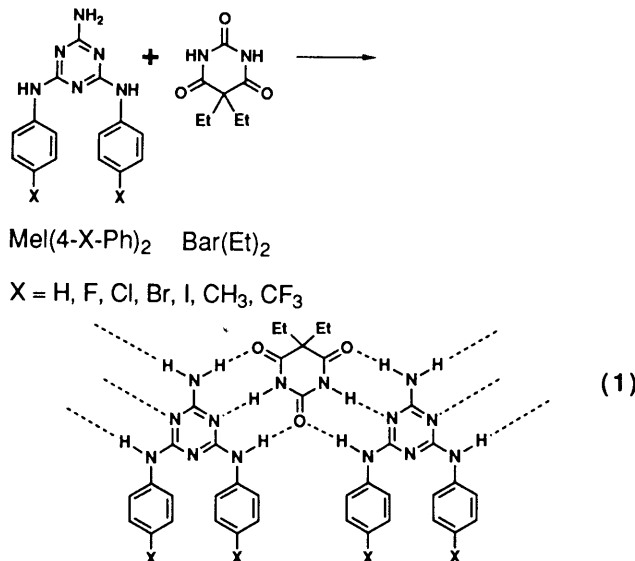
**Abstract:** This paper describes the single-crystal X-ray structures of 1:1 complexes between seven *N,N'*-bis(4-X-phenyl)melamines ( $X = H, F, Cl, Br, I, CH_3$ , and  $CF_3$ ) and 5,5-diethylbarbituric acid. These complexes crystallize as infinite tapes having components joined by triads of hydrogen bonds; the tapes pack with their long axes parallel. The crystalline architecture of these complexes—parallel tapes—serves as a structurally constrained framework with which to study physical–organic relationships between the structures of the crystals and the molecules of which they are composed. The complex with  $X = Br$  exists in polymorphic forms. One of the polymorphs is isomorphous to the  $X = Cl$  complex; the other is related to the  $X = I$  complex.

## Introduction

We are interested in three complementary problems in the organic solid state: rationalizing the structures of organic crystals based on the structures of their component molecules; predicting the structures of new molecular crystals; and designing molecules that crystallize in designed arrays. An understanding of intermolecular interactions that is sufficiently detailed to accomplish these objectives would be useful throughout materials science and would contribute to molecular recognition and molecular self-assembly.

The problem of understanding and predicting the packing of organic molecules in crystals, considered in its full generality, is complicated: a very large number of possible arrangements of molecules in the crystal need to be considered, the differences in energy between crystal forms may be small, and there are no search routines to identify the most stable of these forms.<sup>1</sup> We simplify the problem by reducing the number of orientations open to each molecule by forcing them to form “tapes” (which might also be called “rods” or “ribbons”) connected by networks of hydrogen bonds (eq 1). We expect tapes to pack with their long axes parallel, a geometric arrangement likely to minimize free volume.<sup>2</sup> Packing of hydrogen-bonded tapes with axes parallel would necessarily limit their constituent molecules to a set of arrangements in space that is substantially reduced relative to that available, in principle, to molecules with no constraints on their packing.

We have based our design for tapes on the network of hydrogen bonds present in the 1:1 complex of cyanuric acid and melamine (CA·M). We and others believe that this material has the structure shown in Figure 1, although it has not been possible to grow single crystals of this compound large enough for X-ray diffraction.<sup>3–5</sup> By interrupting the hydrogen bonds (either by replacement of two of the  $NH_2$  groups of melamine with  $NHR$  groups, by substitution of  $NH$  groups in cyanuric acid with  $CR_2$



or  $NR$  groups, or by more complex structural modifications) it is possible to construct at least two types of tape (“linear” and “crinkled”, Figure 1) that preserve the three hydrogen bonds between the two components.<sup>6,7</sup> The objective of the research reported in this paper was to establish the correctness of the hypothesis that molecules of types  $Mel(4-X-Ph)_2$  and  $Bar(Et)_2$  would form 1:1 complexes with tape structures in the solid state. An additional goal was to define the generality of tape formation for a range of substituents on melamines and barbiturates. Our immediate interest was to define structures of a series of molecular crystals differing only in substitution at one position. This set of structures might serve as a starting point for a systematic physical–organic analysis of the relation of molecular to crystal structure.

(5) We consider a crystal to be big enough to warrant investigation using a rotating anode X-ray generator if its smallest dimension is at least 0.05 mm. A crystal referred to in the text as “good” or “usable” or “diffraction quality” was in this size range and was free of cracks or visible twinning under a microscope.

(6) Zerkowski, J. A.; Seto, C. T.; Whitesides, G. M. *J. Am. Chem. Soc.* **1992**, *114*, 5473.

(7) Figure 1 indicates that a possible geometry for a 1:1 complex of  $Mel(4-X-Ph)_2$  and  $Bar(Et)_2$  could also be a cyclic structure  $(Mel(4-X-Ph)_2)_3 \cdot (Bar(Et)_2)_3$ . For  $X = C(CH_3)_3$ , we have observed this disk shape as a crystallographic motif.<sup>6</sup>

\* Abstract published in *Advance ACS Abstracts*, February 15, 1994.  
 (1) Promising approaches for predicting packing have been reported by: Gavezzotti, A. *J. Am. Chem. Soc.* **1991**, *113*, 4622. Perlstein, J. *J. Am. Chem. Soc.* **1992**, *114*, 1955.

(2) We relate our argument for parallel packing of tapes to the similar packing of long-chain alkanes. For a summary, see: Kitaigorodskii, A. I. *Molecular Crystals and Molecules*; Academic Press: New York, 1973.

(3) Seto, C. T.; Whitesides, G. M. *J. Am. Chem. Soc.* **1990**, *112*, 6409.

(4) There is probably substantial disorder in samples of CA·M, and it is difficult to control its nucleation and subsequent crystal growth.

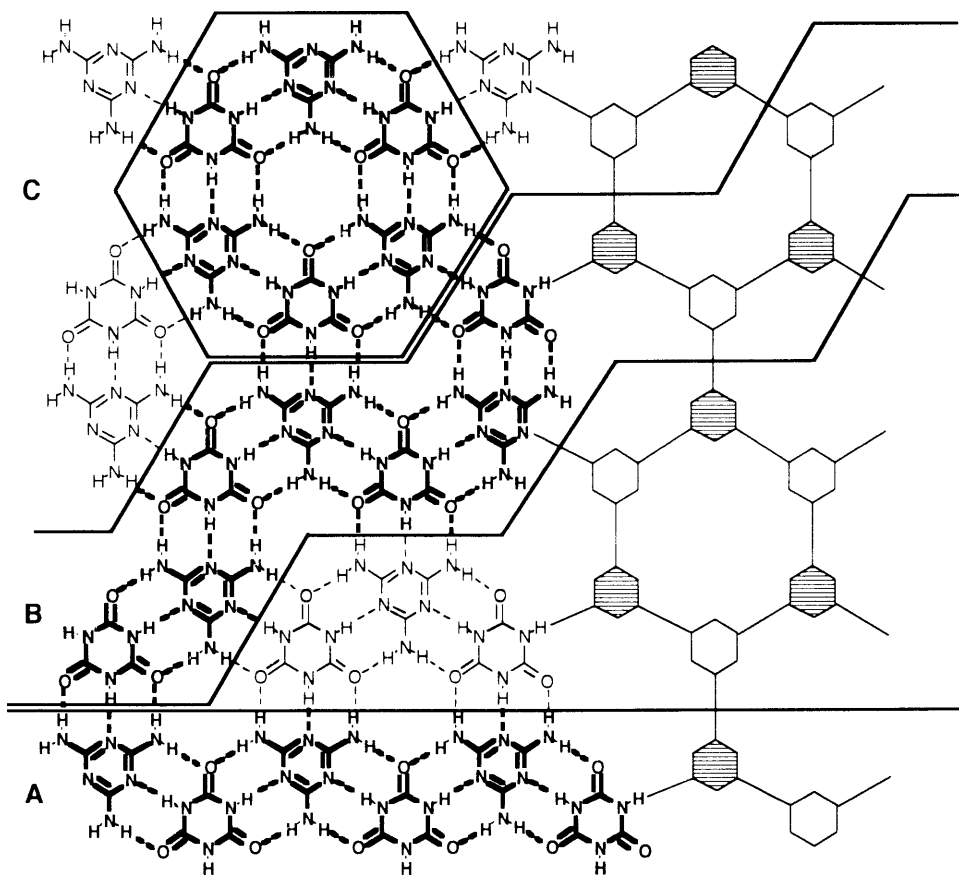


**Figure 1.** Proposed sheet structure of the cyanuric acid·melamine complex. Outlined sections indicate (A) linear tape, (B) crinkled tape, and (C) cyclic hexamer.

**Advantages to the Use of Hydrogen Bonding of Melamines and Barbiturates in Crystal Engineering.** Hydrogen bonds are well suited for use in the design of molecular solids for two reasons: they are directional, and their formation is reversible at room temperature. Using nondirectional forces (e.g. van der Waals and ionic interactions), it is difficult to predict geometries relating adjacent molecules in a crystal. Statistical studies of hydrogen bonds in organic crystals have shown that, for many hydrogen-bonding moieties, bond angles and distances involving the hydrogen atoms and donor and acceptor heteroatoms cluster in a small spread of values.<sup>8</sup> Measurements of the enthalpy of formation of hydrogen bonds in purine and pyrimidine bases—compounds similar to cyanuric acid, barbituric acid, and melamine—and in other compounds give a range of values,<sup>9</sup> but regardless of the precise energetics, hydrogen bonds will be important intermolecular interactions in the solid state.<sup>10</sup> Etter has suggested that strong hydrogen bond donors and acceptors

will always engage in hydrogen bonding in organic solids.<sup>11</sup> Given the directional preferences and strength of hydrogen bonds and the complementary donor/acceptor pattern of melamines and barbiturates, we expect our tapes to assemble reliably.

A further advantage of compounds of the type  $\text{Mel}(4\text{-X-Ph})_2$  and  $\text{Bar}(\text{Et})_2$  is that their heterocyclic core is rigid. Thus, the bidirectional hydrogen bonding necessary for construction of extended solid-state structures is not dependent on conformations of flexible linkers.<sup>12</sup> Their simple trigonal shapes also require consideration of only a few orientations of hydrogen-bonding moieties; this symmetry simplifies predictions of packing.

The syntheses of  $\text{Mel}(4\text{-X-Ph})_2$  and  $\text{Bar}(\text{Et})_2$  are straightforward. We have used barbiturates rather than isocyanurates<sup>13</sup> because the latter have not yielded crystals suitable for single-crystal X-ray analysis.<sup>5,14</sup> The barbiturates seem to be more soluble than isocyanurates in common organic solvents, and the two sites for substitution in the 5-position allow more opportunity for modification.

(8) Taylor, R.; Kennard, O. *Acc. Chem. Res.* **1984**, *17*, 320. Murray-Rust, P.; Glusker, J. P. *J. Am. Chem. Soc.* **1984**, *106*, 1018. Taylor, R.; Kennard, O.; Versichel, W. *Acta Crystallogr.* **1984**, *B40*, 280. Vedani, A.; Dunitz, J. D. *J. Am. Chem. Soc.* **1985**, *107*, 7653.

(9) Calorimetric measurements of association of guanosine and cytidine (derivatized at the 3'- and 5'-positions with triisopropylsilyl groups) in o-dichlorobenzene:  $\Delta H = -2.2 \text{ kcal/mol H-bonds}$ . Williams, L. D.; Chawla, B.; Shaw, B. R. *Biopolymers* **1987**, *26*, 591. Monte-Carlo calculations on G-C base-pair formation in  $\text{CCl}_4$ :  $\Delta E = -5.9 \text{ kcal/mol H-bonds}$ . Pohorille, A.; Burt, S. K.; MacElroy, R. D. *J. Am. Chem. Soc.* **1984**, *106*, 402. Spectrophotometric measurement by van't Hoff analysis of cyclic intramolecular hydrogen bonding in an amide:  $\Delta H = -1.4$  to  $-1.6 \text{ kcal/mol H-bonds}$ . Gellman, S. H.; Dado, G. P.; Liang, G.-B.; Adams, B. R. *J. Am. Chem. Soc.* **1991**, *113*, 1164. Calculations using thermodynamic cycles based on estimates for translational and rotational entropies:  $\Delta H \approx -2.9 \text{ kcal/mol H-bonds}$  (mean in  $\text{CCl}_4$ ) and  $-1.0 \text{ kcal/mol H-bonds}$  (mean in  $\text{H}_2\text{O}$ ). Doig, A. J.; Williams, D. H. *J. Am. Chem. Soc.* **1992**, *114*, 338. Measurements of differential binding of substrates to enzymes in the presence and absence of hydrogen-bonding groups:  $\Delta G = -0.5$  to  $-1.8 \text{ kcal/mol H-bonds}$ . Fersht, A. R. *Trends Biochem. Sci.* **1987**, *12*, 301.

(10) Desiraju, G. R. *Crystal Engineering: The Design of Organic Solids*; Elsevier: New York, 1989.

(11) Etter, M. C. *J. Am. Chem. Soc.* **1982**, *104*, 1095. There are exceptions to this guideline; see the structure of alloxan, which engages in only weak, bifurcated hydrogen bonds: Swaminathan, S.; Craven, B. M.; McMullan, R. K. *Acta Crystallogr.* **1985**, *B41*, 113.

(12) Garcia-Tellado, F.; Geib, S. J.; Goswami, S.; Hamilton, A. D. *J. Am. Chem. Soc.* **1991**, *113*, 9265. Etter, M. C.; Adsmond, D. A. *J. Chem. Soc., Chem. Commun.* **1990**, 589.

(13) Isocyanurates are N-alkylated; cyanurates are O-alkylated. Following this convention, the parent molecule as its trishydroxy tautomer should be named cyanuric acid, even though it is known to exist almost exclusively as the triketo form. Our examination of the literature suggests that the name isocyanuric acid is rarely used, however, so we will continue to refer to the triketo form as cyanuric acid.

(14) We suspect that the greater acidity of isocyanurates relative to barbiturates may lead to stronger hydrogen bonding along one developing crystalline axis in the former case and hence to rapid and uncontrollable crystal growth. Isocyanurates were also more difficult to synthesize. Perrin, D. D. *Dissociation Constants of Organic Bases in Aqueous Solution*; Butterworths: London, 1965.

**Precedent for Crystal Engineering of Hydrogen-Bonded Structures.** Infinite chains based on hydrogen bonds have been observed and studied previously, notably in monocomponent crystals of amides and carboxylic acids. Leiserowitz and colleagues have produced comprehensive catalogues of crystalline features arising from hydrogen bonding of these functionalities.<sup>15</sup> The relationships between the molecular structures of alicyclic diols and their packing motifs have been investigated by Bishop and Dance.<sup>16</sup> Etter's work provides useful structural generalizations and predictive guidelines for patterns of solid-state hydrogen-bonded networks.<sup>17</sup> Several hydrogen-bonded dimers of barbiturates have been reported by Craven,<sup>18</sup> and Shimizu has observed a hydrogen-bonded chain of barbital cocrystallized with adenine.<sup>19</sup> Lehn has examined a molecular tape similar to ours<sup>20</sup> and has used hydrogen bonds to design other kinds of systems.<sup>21</sup>

**Guide to the Work.** The data presented below support our hypothesis that threefold hydrogen bonding leads to the formation of crystalline tapes. These tapes consist of a structurally constant backbone and variable periphery that can be altered by substitution on Mel(4-X-Ph)<sub>2</sub> and barbiturates. The packing of the tapes is sensitive to small perturbations on the molecular composition. In at least two cases ( $X = \text{Br}$  and  $\text{CF}_3$ ) polymorphism occurs, allowing packing of a complex in more than one phase.<sup>22</sup> Despite the complexity introduced by polymorphism, we believe that this system of linear, hydrogen-bonded tapes is an excellent one with which to study the physical-organic chemistry of organic molecular solids. Its most serious shortcomings at present are that numerous crystallization efforts may be required to obtain single crystals large enough for X-ray analysis, that polymorphism complicates interpretation, and that difficulties may be encountered in forming single crystals containing certain polar substituents.

## Results

**Crystallizations.** We have not yet developed a single crystallization procedure that produces diffraction-quality single crystals of tapes. An acicular crystal habit was the one most frequently obtained. The most common reason for rejecting a batch of crystals was that the needles were too thin.<sup>5</sup> We suggest that the crystals grow rapidly in the direction of faces that expose hydrogen bonds. A solvent capable of both donating and accepting hydrogen bonds should, in principle, bind well to the crystal face exposing polar hydrogen-bonding moieties and should slow growth in this direction, while allowing growth to continue on faces with exposed alkyl or aryl substituents.<sup>23</sup> Crystals that are less acicular are in fact obtained from methanol and ethanol, while solvents of lesser hydrogen-bonding ability gave whiskers. Thus one

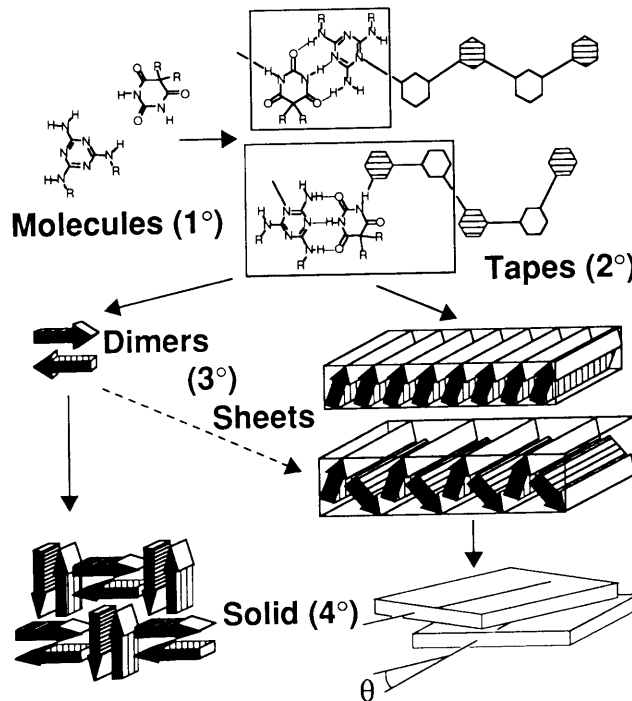


**Figure 2.** Hierarchies of structural elements, or crystalline architecture, in crystals of the 1:1 complexes of  $N,N'$ -bis(4-X-phenyl)melamines and 5,5-diethylbarbituric acid. Levels of structural organization are suggested schematically: primary =  $1^\circ$ , molecules; secondary =  $2^\circ$ , tapes; tertiary =  $3^\circ$ , arrays of tapes with parallel axes; quaternary =  $4^\circ$ , full solid, axes of tapes may be nonparallel.

guideline that we can offer is that hydrogen-bonding solvents work best for crystallizations of solutes of this sort.<sup>24</sup> Indexing of crystal faces, to allow correlation of the tape packing direction with the shape of the crystal, has been performed in only one case (on the  $\text{Mel}(4\text{-F-Ph})_2\text{-Bar}(\text{Et})_2$  complex). The long needle axis did correspond with the long tape axis, along the crystallographic  $b$  direction, in that case.<sup>25</sup>

**Structural Generalizations.** As background for the experimental results, we summarize two limitations (summarized graphically in Figure 2) to the types of structures considered. First, we consider only linear tapes; crinkled tapes have also been observed.<sup>6</sup> Limiting consideration to the linear tapes allows us to focus on the structural features common to them. Second, we further restrict the scope of this paper to small structural perturbations generated by a series of substituents in the *para* position of the phenyl rings of  $N,N'$ -diphenylmelamines: H, F, Cl, Br, I,  $\text{CH}_3$ , and  $\text{CF}_3$ . For all of these structures,  $\theta$  (Figure 2, bottom) is zero: that is, all the tapes pack with their long axes parallel.<sup>26</sup> A conglomerate view of all these substituents, showing their relative van der Waals radii, is presented in Figure 3.

**Solid-State Structures of Complexes  $\text{Mel}(4\text{-X-Ph})_2\text{-Bar}(\text{Et})_2$ .** Figures 4–11 summarize the structures of 1:1 cocrystals between 5,5-diethylbarbituric acid ( $\text{Bar}(\text{Et})_2$ ) and derivatives of diphen-

- (15) Leiserowitz, L.; Hagler, A. T. *Proc. R. Soc. London* **1983**, *A388*, 133.
- Leiserowitz, L. *Acta Crystallogr.* **1976**, *B32*, 775.
- (16) Bishop, R.; Dance, I. G. in *Inclusion Compounds*; Atwood, J. L., MacNicol, D. D., Davies, J. E. D., Eds.; Academic Press: London, 1991; Vol. IV.
- (17) Etter, M. C. *Acc. Chem. Res.* **1990**, *23*, 120.
- (18) Hsu, I.; Craven, B. M. *Acta Crystallogr.* **1974**, *B30*, 974.
- (19) Shimizu, N.; Nishigaki, S.; Nakai, Y.; Osaki, K. *Acta Crystallogr.* **1982**, *B38*, 2309.
- (20) Lehn, J.-M.; Mascal, M.; DeCian, A.; Fischer, J. *J. Chem. Soc., Perkin Trans. 2* **1992**, 461.
- (21) Lehn, J.-M. *Angew. Chem., Int. Ed. Engl.* **1990**, *29*, 1304.

(22) A systematic study of the crystal packing of organic molecules must take polymorphism into consideration. We have found that at least two members of this family of complexes,  $\text{Mel}(4\text{-Br-Ph})_2\text{-Bar}(\text{Et})_2$  and  $\text{Mel}(4\text{-CF}_3\text{-Ph})_2\text{-Bar}(\text{Et})_2$ , display polymorphism. For  $X = \text{Br}$ , we observe three polymorphs. The structures of two are reported here, but we have been unable to obtain large enough crystals of the third for single-crystal analysis. For  $X = \text{CF}_3$ , we observe two polymorphs, the one for which we have obtained good crystals is described here. A full investigation of the alternative packing modes of the *para* series of complexes, relying on X-ray powder diffraction and solid-state NMR, will be presented in a separate publication.

(23) Berkovitch-Yellin, Z.; van Mil, J.; Addadi, L.; Idelson, M.; Lahav, M.; Leiserowitz, L. *J. Am. Chem. Soc.* **1985**, *107*, 3111. Wierko, F. C.; Shimon, L. J. W.; Frolow, F.; Berkovitch-Yellin, Z.; Lahav, M.; Leiserowitz, L. *J. Phys. Chem.* **1987**, *91*, 472. Wang, J.-L.; Leiserowitz, L.; Lahav, M. *J. Phys. Chem.* **1992**, *96*, 15.

(24) Broader generalizations on the techniques we have used will be published at a later time. The crystals discussed in this work, except for the fluorine-containing complexes, were comparatively readily grown; that is, they did not require many trial-and-error-based crystallization attempts. We have not been able to crystallize melamines with polar substituents (e.g.  $\text{CO}_2\text{H}$ ,  $\text{CONH}_2$ , or  $\text{CN}$ ). After several attempts, we could only obtain microcrystals, at best. We suspect that the need for these substituents to hydrogen bond may be geometrically incompatible with close packing of tapes.

(25) The data collected from the particular crystal that was indexed gave a crystallographic solution that could not be refined below an  $R$ -factor of 0.20. Since a recollection of data from another crystal gave an essentially identical solution (and good refinement), we do believe that the tape/needle correspondence is real.

(26) Strong interactions between tapes might, however, make  $\theta \neq 0$ . This is the case in the complex between melamine and barbituric acid, where three-dimensional hydrogen bonding of tapes twists  $\theta$  to almost 90°. Zerkowski, J. A.; Whitesides, G. M. Unpublished results.

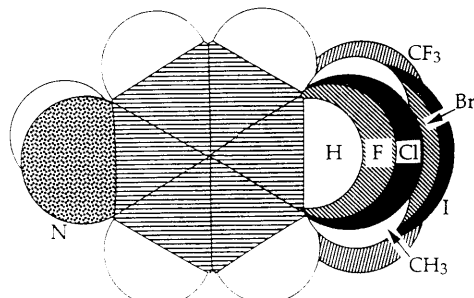


**Figure 3.** Comparative van der Waals sizes of the phenyl substituents used in this work. The van der Waals radii used are listed in ref 29. The NH group *para* to the substituents is attached to the triazine ring.

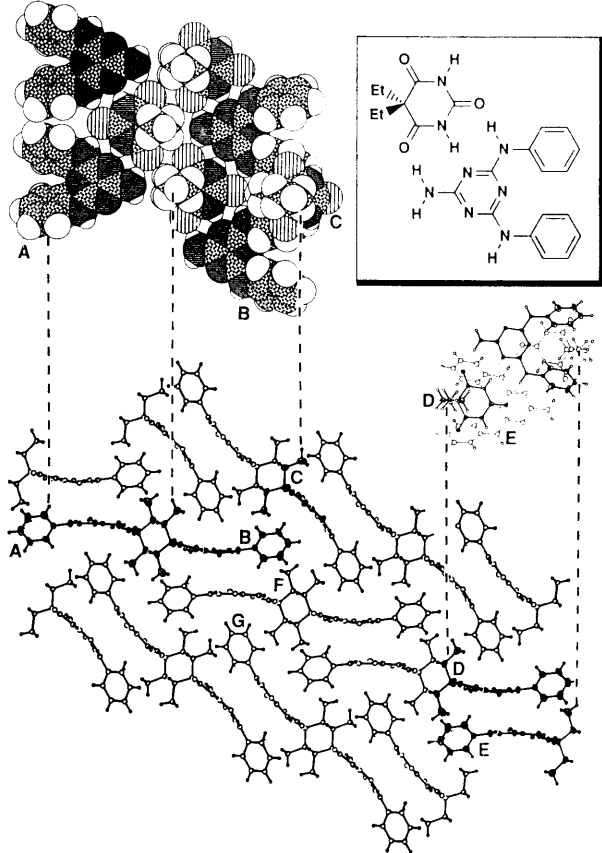


**Figure 4.** Views of the  $\text{Mel}(4\text{-H-Ph})_2\text{·Bar}(\text{Et})_2$  complex.

ylmelamine substituted in the *para* position with substituents X ( $\text{Mel}(4\text{-X-Ph})_2$ ). These figures show several views of packing at once and are intended to provide the information needed to discuss packing. We are primarily concerned here with *intermolecular* interactions. We have not yet found a single representation of the crystal structure that provides the information needed to visualize intertape, contacting van der Waals surfaces. Stereoscopic views are not helpful. The sets of composite views given in Figures 4–11, while complicated, represent the most useful way we have developed to describe packing and to show close, nonbonded contacts between molecules.

The central portion of each figure shows an end-on view, looking down the long axes of the tapes. This view illustrates the major stacking motifs of the tapes. Both the van der Waals section and the remaining ball-and-stick picture(s) are views looking down on selected tapes (indicated in the end-on view with thermal ellipsoids). The vertical dotted lines identify tapes that appear in more than one view. The letters also identify corresponding structures in different views. The ball-and-stick top-down view shows how various portions of the tapes overlap. For simplicity, the only noncovalent interactions illustrated (dotted lines) are hydrogen bonds.

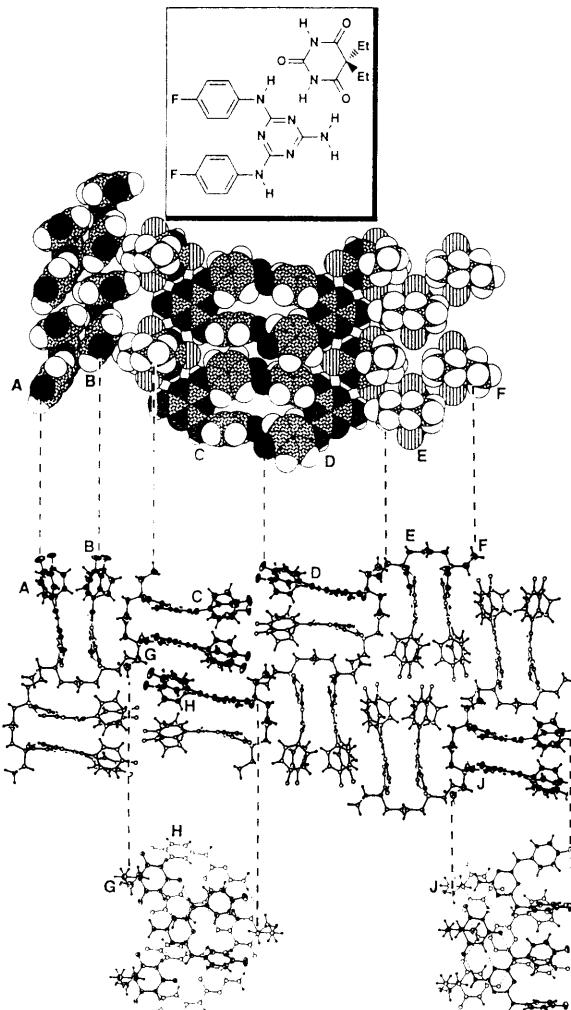


**Figure 5.** Views of the  $\text{Mel}(4\text{-F-Ph})_2\text{·Bar}(\text{Et})_2$  complex.

To summarize the registry of the tapes along their long axes, we introduce the symbolism shown in Figure 12. We choose one tape (A, Figure 12), arbitrarily as a reference, and represent its orientation in the crystal by an arrow attached to an open circle. All the other tapes represented by open circles are related to the reference tape by simple translation perpendicular to the long axis of the tape. The relation of any other tape (B, Figure 12) to the reference tape is determined by the manipulations that must be performed to superimpose it on the reference tape. First, we move tape B along the tape axis (and in the positive direction of the parallel crystallographic axis) by a distance  $\lambda$  (see Figure 12) until its melamine and barbiturate groups (but not necessarily the substituents on these groups)<sup>27</sup> line up with those of the reference tape. To convert the fraction  $\lambda/L$  (where  $L$  is the repeat distance along a tape axis, Figure 13) to a graphic symbol, we multiply by  $2\pi$  radians and represent the resulting angle  $\varphi$  on the circle attached to the arrow representing tape B. Other manipulations of tape B required to superimpose it on tape A—reflections of melamine and barbiturate units across a mirror plane perpendicular or parallel to the long axis—are also indicated in Figure 12.

The most important information summarized in Figure 12 is the relative positions and orientations of the tapes. Thus, for example, X = Cl and X = Br (form I) are isomorphous,<sup>28</sup> and

(27) Since the angles at the melamine nitrogens linking the phenyl ring to the triazine ring are greater than  $120^\circ$  (Figure 13) and are not equal to each other, the phenyl rings splay out and the intramolecular separation of the *para* substituents is greater than the width of the triazine ring. Thus depending on the crystallographic relationship of two tapes, superimposing their backbones might not superimpose their substituents.

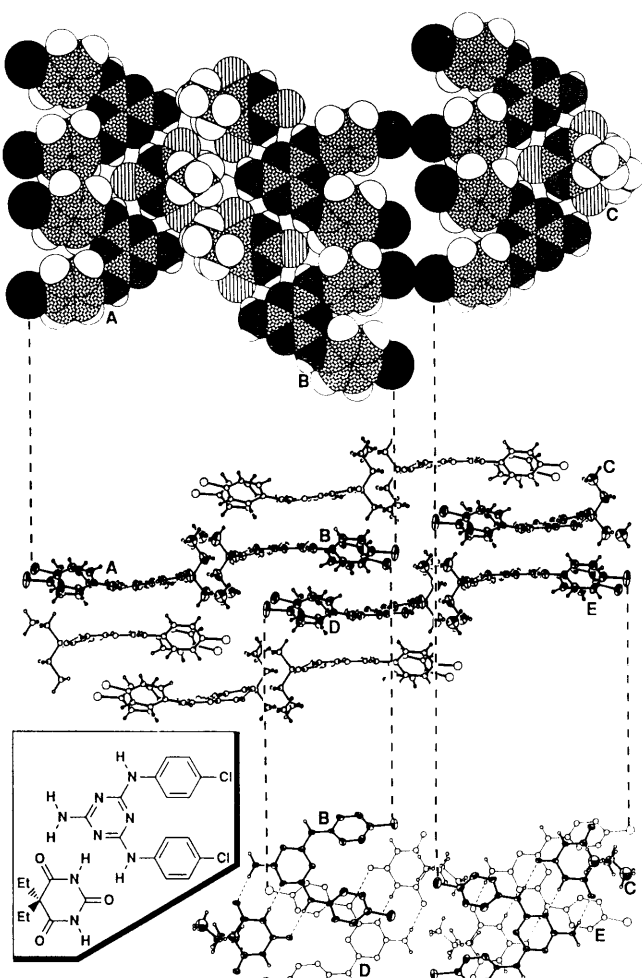


**Figure 6.** Views of the  $\text{Mel}(4\text{-Cl-Ph})_2\text{-Bar}(\text{Et})_2$  complex. Only one orientation of the disordered ethyl groups of barbital is shown.

$X = \text{I}$ ,  $X = \text{CH}_3$ , and  $X = \text{Br}$  (form II) are a closely related set. Head-to-tail dimers occur in four structures (H, Cl, Br (form I), and  $\text{CF}_3$ ). The tape with  $X = \text{F}$  is unique in its architecture. Table 1 lists some pertinent crystallographic data.

**$N,N'$ -Diphenylmelamine/barbital ( $\text{Mel}(4\text{-H-Ph})_2\text{-Bar}(\text{Et})_2$ ).** The phenyl and ethyl substituents on adjacent, stacked tapes dovetail: tapes D and E (a centrosymmetric dimer) in Figure 4 show how the phenyl groups of one tape in an inversion-related pair of tapes tilt to form a small pocket into which an ethyl group from the partner tape can fit. This kind of accommodation is repeated between nonparallel tapes, as between tapes B and C in Figures 4 and 14. There are no intertape phenyl–phenyl interactions, such as in a stacking or edge-to-face arrangement.

**$N,N'$ -Bis(4-fluorophenyl)melamine/barbital ( $\text{Mel}(4\text{-F-Ph})_2\text{-Bar}(\text{Et})_2$ ).** There are two dimers in the asymmetric unit of this complex. The packing is built up from both centrosymmetric, or head-to-tail dimers (tapes G and H in Figure 5), and parallel head-to-head dimers (tapes C and G). The interplanar separations between the head-to-head tapes are smaller than those for the head-to-tail tapes (3.3–3.5 vs 4.2–4.4 Å). There are no fluorine–fluorine contacts, but there is a hydrogen–fluorine contact: one fluorine atom in tape C is 2.44 Å away from a *meta*-phenyl hydrogen in tape D ( $\Sigma_{\text{vdW}} \approx 2.67$  Å).<sup>29–31</sup> One of the ethyl groups

(28) “Crystals in which the atomic positions are essentially the same but differ only in the nature of the atoms that occupy these positions are called isomorphous; ...they are recognized by their similar cell dimensions, same space group, and similar diffraction patterns.” Dunitz, J. D. *X-Ray Analysis and the Structure of Organic Molecules*; Cornell University Press: Ithaca, NY, 1979; p 123.

(29) We are using isotropic van der Waals radii: H, 1.20 Å; C, 1.70 Å; N, 1.55 Å; O, 1.52 Å; F, 1.47 Å; Cl, 1.75 Å; Br, 1.85 Å; I, 1.98 Å. Bondi, A. *J. Phys. Chem.* 1964, 68, 441. For anisotropic van der Waals radii, see: Nyburg, S. C.; Faerman, C. H. *Acta Crystallogr.* 1985, B41, 274.

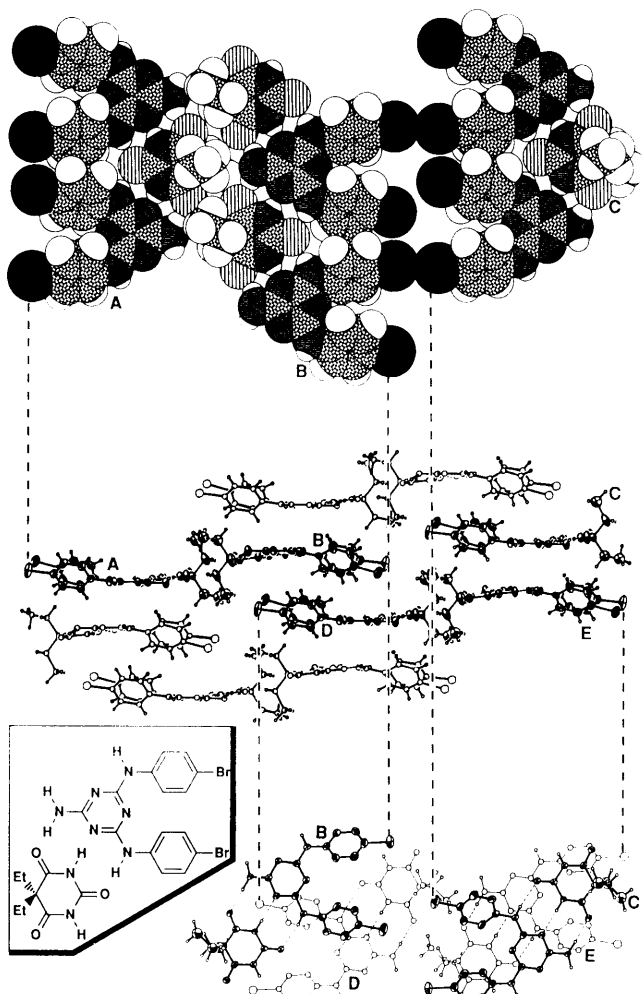


**Figure 7.** Views of the  $\text{Mel}(4\text{-Br-Ph})_2\text{-Bar}(\text{Et})_2$  (form I) complex. Only one orientation of the disordered ethyl groups of barbital is shown.

is disordered, with the methyl group occupying two different positions in approximately a 2:1 ratio.

**$N,N'$ -Bis(4-chlorophenyl)melamine/barbital and  $N,N'$ -Bis(4-bromophenyl)melamine/barbital ( $\text{Mel}(4\text{-Cl-Ph})_2\text{-Bar}(\text{Et})_2$  and  $\text{Mel}(4\text{-Br-Ph})_2\text{-Bar}(\text{Et})_2$  (Form I)).** These complexes are isomorphous. The centrosymmetric dimer is again a principal motif. Both ethyl groups of barbital are disordered. In both complexes, there are no halogen–halogen contacts at or under the sum of the van der Waals radii.

**$N,N'$ -Bis(4-iodophenyl)melamine/barbital and  $N,N'$ -Bis(4-bromophenyl)melamine/barbital ( $\text{Mel}(4\text{-I-Ph})_2\text{-Bar}(\text{Et})_2$ ) and  $\text{Mel}(4\text{-Br-Ph})_2\text{-Bar}(\text{Et})_2$  (Form II)).** The halogen–halogen interactions are more extensive in these complexes than in those for which  $X = \text{F}$ , Cl, and Br (form I) and are clearly less than the sum of van der Waals radii: for iodine,  $\Sigma_{\text{vdW}} \approx 4.0$  Å, I–I contacts at 3.76 and 3.81 Å; for bromine,  $\Sigma_{\text{vdW}} = 3.7$  Å, Br–Br contacts at 3.75 and 3.50 Å. These interactions occur between tapes. The packing has changed to a format based on sheets.

**$N,N'$ -Bis(4-methylphenyl)melamine/barbital ( $\text{Mel}(4\text{-CH}_3\text{-Ph})_2\text{-Bar}(\text{Et})_2$ ).** The packing of this complex is very similar to that of  $\text{Mel}(4\text{-I-Ph})_2\text{-Bar}(\text{Et})_2$  and  $\text{Mel}(4\text{-Br-Ph})_2\text{-Bar}(\text{Et})_2$  (form II), although none of the three are in fact crystallographically

(30) Since we placed all the hydrogen atoms in calculated positions for determining intermolecular contacts, we will only propose that specific contacts involving hydrogens are suggested and will not put too much emphasis on the precise distances of these contacts. Most of the contacts that we comment upon in the text are at least 0.1 Å less than the sum of van der Waals radii of the interacting atoms. We believe, however, that even if a hydrogen–heteroatom contact is slightly over the sum of van der Waals radii, it will still probably play some role in guiding packing.

(31) All aliphatic and aromatic C–H bonds were set to 1.08 Å, and all N–H bonds to 1.00 Å.

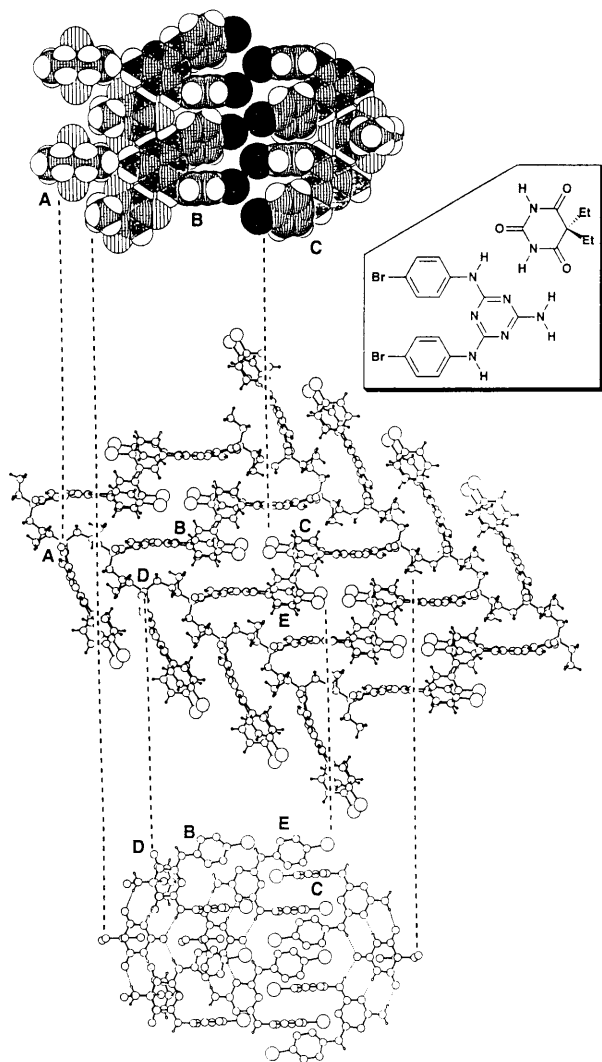


**Figure 8.** Views of the  $\text{Mel}(4\text{-Br-Ph})_2\text{-Bar}(\text{Et})_2$  (form II) complex.

isomorphous. Between the methyl groups, there are no intertape contacts analogous to the halogen-halogen interactions of the preceding two  $\text{Mel}(4\text{-X-Ph})_2\text{-Bar}(\text{Et})_2$  complexes.

**$N,N'$ -Bis(4-trifluoromethylphenyl)melamine/barbital ( $\text{Mel}(4\text{-CF}_3\text{-Ph})_2\text{-Bar}(\text{Et})_2$ ).** There is rotational disorder around the  $\text{F}_3\text{C-C}_{\text{aryl}}$  bond. Intertape fluorine-hydrogen contacts at 2.41, 2.45, and 2.51 Å ( $\Sigma_{\text{vdW}} \approx 2.67$  Å) exist between the fluorines of tape D and the barbital  $\text{CH}_3$  hydrogens of tape C in Figure 11, although the disorder cautions against overinterpreting those contacts. There are no fluorine-fluorine interactions.

**Packing Fractions.** Table 1 lists the packing fractions,  $C_k^*$ ,<sup>32</sup> for all the complexes. The packing fraction, which is a measure of the efficiency of space filling in a crystal, is defined by eq 2, where  $V_m$  is the molecular volume,  $N$  is the number of molecules

$$C_k = N(V_m/V_c) \quad (2)$$

in the unit cell (which is not necessarily equal to  $Z$ , the number of asymmetric units), and  $V_c$  is the volume of the unit cell. The molecular volumes were calculated by putting crystallographic coordinates into MacroModel.<sup>33</sup> All C-H and N-H bond lengths were set to conventional values.<sup>31</sup> The MacroModel volume-calculating facility was used without alteration, so these values, while in the acceptable range for organic compounds, are not intended for comparison to previous literature values for  $C_k$ .<sup>34</sup> We have therefore employed a modified label,  $C_k^*$ , for the packing

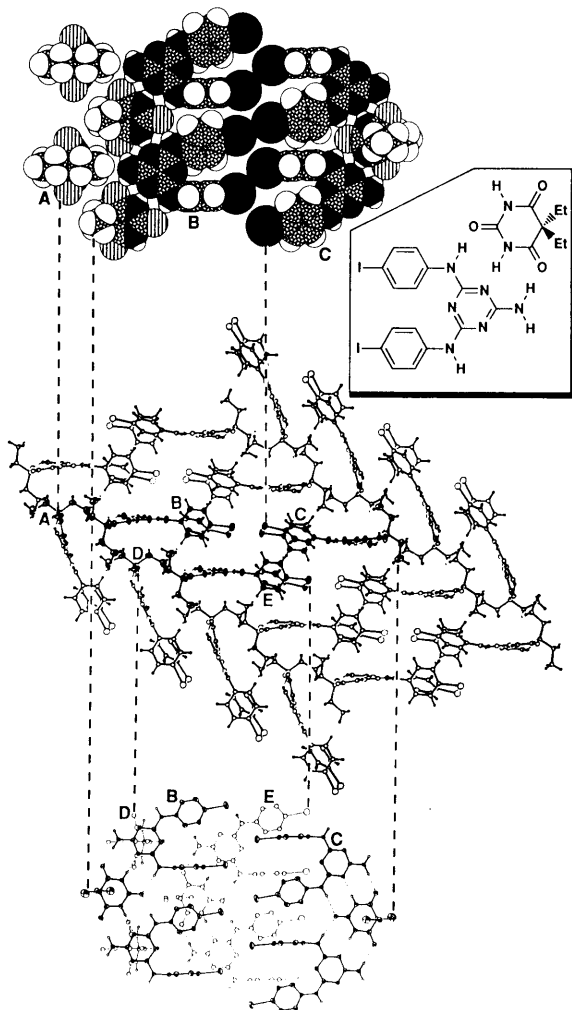


**Figure 9.** Views of the  $\text{Mel}(4\text{-I-Ph})_2\text{-Bar}(\text{Et})_2$  complex.

fraction. Furthermore, strict comparisons should only be made for structures done at the same temperature ( $X = \text{F}, \text{Cl}, \text{Br}$  (forms I and II), I, and  $\text{CF}_3$ ).

Regarding the two  $X = \text{Br}$  polymorphs, Kitaigorodskii's close-packing principle would suggest that the form I polymorph should be the more thermodynamically stable, since it fills space more efficiently and since there are no strong directional intertape interactions.<sup>2,10</sup> The disordered ethyl groups should also favor this polymorph by raising the entropy of the crystal. A complete discussion of the relative energetics of these two polymorphs must await detailed calculations.<sup>22</sup>

The lowest packing coefficient, that for  $\text{Mel}(4\text{-CF}_3\text{-Ph})_2\text{-Bar}(\text{Et})_2$ , is consistent with the existence of rotational disorder in the

(34) We calculated some molecular volumes using published crystallographic coordinates to compare our MacroModel-derived packing fractions to literature values (compound and reference for crystallographic coordinates, literature value for  $C_k$  and reference, our MacroModel value for  $C_k^*$ ): hexanitrobenzene (ref 34a), 0.64 (ref 2), 0.68; hexacyanobenzene (ref 34b), 0.56 (ref 10), 0.61; resorcinol,  $\alpha$ -form (ref 34c), 0.67 (ref 32), 0.68; acridine (ref 34d), 0.71 (ref 32), 0.73. (a) Akopyan, Z. A.; Struchkov, Yu. T.; Dashevskii, V. G. *Zh. Strukt. Khim.* **1966**, 7, 408. (b) Drück, U.; Kutoglu, A. *Acta Crystallogr.* **1983**, C39, 638. (c) Robertson, J. M. *Proc. R. Soc. 1936*, A157, 79. (d) Phillips, D. C. *Acta Crystallogr.* **1956**, 9, 237. The values of  $C_k$  that come from Kitaigorodskii's work<sup>2,10</sup> were almost certainly calculated from tables of average volume increments, since Kitaigorodskii developed and promoted that method. Obvious drawbacks to his approach are that some functional groups may not have tabulated values and that different volume contributions may be inferred from different molecular environments. While some of these pairs of  $C_k$  and  $C_k^*$  values may not be as close to each other as is desirable, the relative ease of calculating molecular volumes using MacroModel or some other widely accessible program recommends our procedure. As long as the programs use the same set of van der Waals radii,<sup>29</sup> comparisons should be valid. We hope that this approach, rather than the use of potentially antiquated or incomplete tables of volume increments for functional groups,<sup>2,32</sup> may induce wider reporting of packing fractions.

(32) Kitaigorodskii, A. I. *Organic Chemical Crystallography*; Consultants Bureau: New York, 1961.

(33) Still, W. C., et al. *MacroModel V3.0*; Department of Chemistry, Columbia University: New York, 1990.

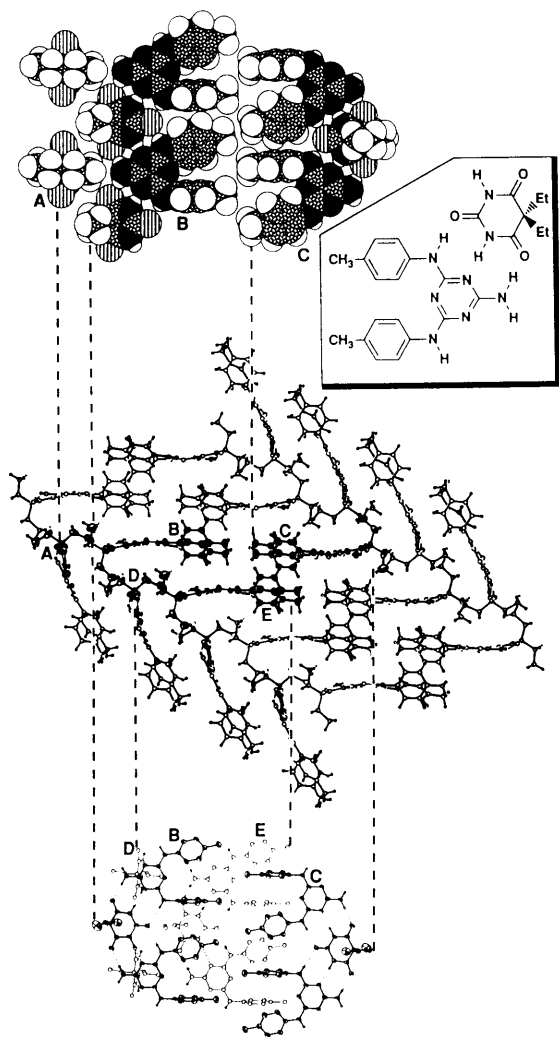


**Figure 10.** Views of the  $\text{MeI}(4\text{-CH}_3\text{-Ph})_2\text{-Bar}(\text{Et})_2$  complex.

$\text{CF}_3$  groups. If packing is loose, there may be enough free space to permit molecular motion in the crystal.<sup>35</sup> There is no correlation between substituent size and tightness of packing.

## Discussion

The eight structures described here confirm the hypothesis that suitably designed 1:1 cocrystals of  $N,N'$ -disubstituted melamines and dialkylbarbituric acids form linear tapes in the solid state. These structures all have relatively small, nonpolar substituents in the 4-position of the phenyl groups of  $N,N'$ -diphenylmelamine. Larger, nonpolar substituents ( $\text{CO}_2\text{CH}_3$ , *tert*-butyl) lead to different structures (crinkled tapes or cyclic "rosettes"); these structures have been described in a separate paper.<sup>6</sup> We have not yet been able to prepare cocrystals suitable for single-crystal X-ray diffraction when the substituent in the 4-position is polar ( $\text{CO}_2\text{H}$ , CN,  $\text{CONH}_2$ ).

The limitation to the formation of linear tapes in the structural class of cocrystals explored here appears to be unfavorable steric interactions between the substituents in the 4-positions of phenyl groups of *adjacent* melamines (Figure 13, Table 2). The intermolecular separation of substituents ( $d$  in Figure 13) is always smaller than the intramolecular separation ( $d'$ ). This feature reflects the fact that the angle at the melamine nitrogen connecting the phenyl and triazine rings ( $\Phi$  in Figure 13) is greater than  $120^\circ$ . For the larger  $X$  groups  $\text{CH}_3$  and  $\text{CF}_3$ ,  $d$  is smaller than

(35) A reviewer has pointed out that it is the *local*, not the overall, packing efficiency near a disordered group that is relevant to its disorder. Nonetheless, it seems reasonable to expect that local regions of loose packing may contribute to a reduced overall packing fraction.

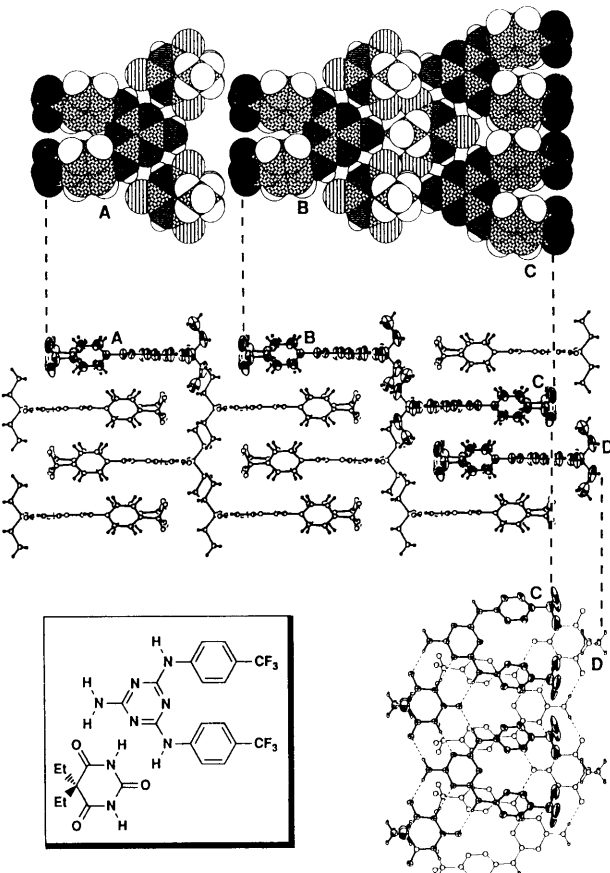


**Figure 11.** Views of the  $\text{MeI}(4\text{-CF}_3\text{-Ph})_2\text{-Bar}(\text{Et})_2$  complex. Only one orientation of the disordered trifluoromethyl group is shown.

the van der Waals diameter of  $X$ . Since these diameters assume a semicircular cross section, they probably imply a potential for steric repulsion that is greater than that existing between real, noncylindrical  $\text{CH}_3$  or  $\text{CF}_3$  groups. Any increase in the size of  $X$  beyond the values of these larger substituents would lead to repulsive interactions and prevent formation of a linear tape.<sup>7</sup> The quantity  $d + d'$  is constant at about  $10 \text{ \AA}$ , and this value is greater than the translational repeat distance within a tape ( $9.70\text{--}9.98 \text{ \AA}$ , Table 1;  $L$  in Figure 13). This extra separation is attained by a distortion of the phenyl rings above or below the mean planes of the hydrogen-bonded backbones.

When the *para* substituent is bromine, which comes toward the middle of the range of sizes spanned by substituents H to  $\text{CF}_3$  (Table 2), two alternative packing arrangements (at least)<sup>22</sup> are energetically accessible at ambient conditions. Complexes with the smaller substituents H, F, and Cl adopt a packing that is based on dimers of tapes (Figure 2), although the architecture of the case with  $X = \text{F}$  is unique and complicates this simplified picture. Complexes with the larger substituents  $\text{CH}_3$  and I adopt a packing that is sheet-like, although, again, the fluorinated complex with  $X = \text{CF}_3$  does not fit into this picture, since it packs with head-to-tail dimers that are further stacked into sheets (see, however, footnote 22). The complexes with the intermediate-sized  $X = \text{Br}$  substituents can adopt either a dimer-based (Figure 7) or a sheet-based (Figure 8) packing. Thus, as we have observed with bulkier substituents,<sup>6</sup> the steric properties of the substituents in the *para* positions of these diphenylmelamine complexes appear to be critical to determining both secondary and tertiary crystalline architecture.

The overall quality of these structures (as measured by the crystallographic  $R$ -index) varies from 0.04 to 0.09. An independent measure of the reliability of the structures comes from examination of the geometries of the triazine, phenyl, and barbituric groups. These fragments would be expected to be approximately constant in geometry, and errors in the crystal structures might

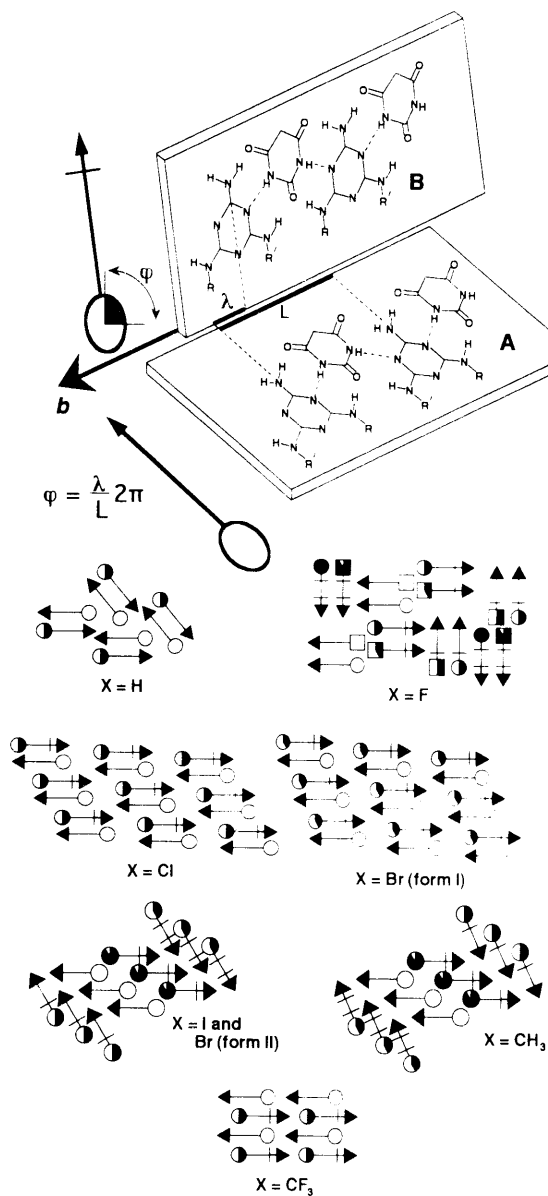


**Figure 12.** Top: Schematic diagram summarizing the packing of tapes. Tape B is moved in the positive direction along its long axis until the atoms of the tape backbones in the two tapes have (in this example) the same  $y$  coordinate.  $\varphi$  (radians) is the fraction of the repeat distance in a tape ( $L$ ) that tape B must be moved to line up with tape A (open circle). The arrows with circles attached represent end-on views of the tapes, looking down their long axes. Bottom: All the tapes with partially filled circles are related to the reference tapes by at least a rotation around an axis parallel to the long tape axis. A crossbar near the arrowhead indicates that a reflection across a mirror plane perpendicular to the long axes must also be done (as in the picture at the top); a crossbar near the circle indicates the same for a mirror plane parallel to the long axes. The reference unit in the  $X = F$  case is a dimer (one circle and one square), since there are two independent tapes in that complex. The offset amount  $\varphi$  is rounded to the nearest twelfth for clarity of the filled circles. This rounding exaggerates the difference between the isomorphous structures  $X = Cl$  and  $Br$  (form I).

be expected to appear as distortions from the anticipated geometries. In fact the observed geometries are sensibly constant.

## Conclusions

The objective of this work was to develop a class of organic crystals that would exist in a limited set of crystalline architectures but would allow the kind of variation in structure useful in physical-organic studies of structure-property relationships. These 1:1 cocrystalline tapes have many of the desired characteristics. Their components are easily synthesized and can be

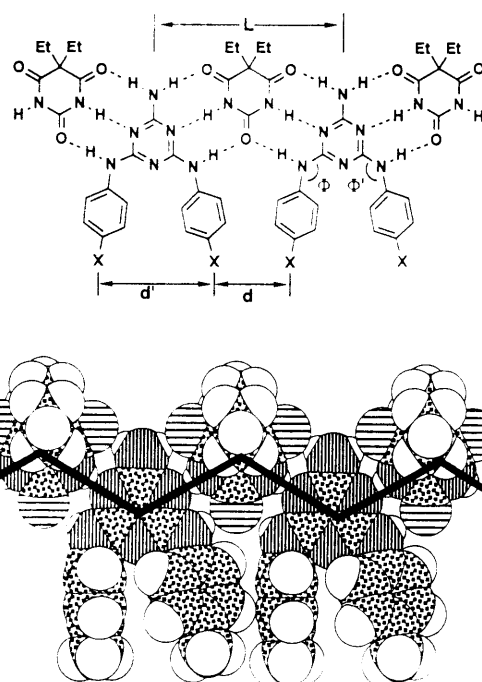


**Figure 13.** Intratape measurements listed in Table 2.  $L$  is the crystallographic repeat in a tape.

varied widely over a range of structures. The observation that linear tapes are frequently obtained, and that these tapes pack with their long axes parallel, has the potential to simplify the analysis of solid-state structure significantly (relative to crystals in which the constituent molecules can, in principle, adopt many conformations with respect to one another).

The system also has three disadvantages: growing crystals of the quality and size suitable for single-crystal X-ray diffraction requires patience; the system has not yet proved amenable to the introduction of polar substituents (perhaps because of competition of these substituents for hydrogen bonding sites); and at least some of the crystals can apparently exist in several crystalline forms. The issue of polymorphism is probably the one with the most far-reaching consequences.<sup>22</sup> Nonetheless, the important feature of our system is that it does tolerate small changes in molecular structure while maintaining a consistent solid-state motif. We have, thus, demonstrated a system that allows systematic investigation into crystalline architecture.

## Experimental Section

**General Methods.** Cyanuric chloride (Fluka), barbital (Fisher Scientific), and all anilines (Aldrich) were used as received without purification. Solvents were reagent grade and were used without purification unless otherwise indicated; THF was distilled from sodium benzophenone ketyl. Melting points were determined on a Mel-Temp apparatus and are uncorrected.

**2-Amino-4,6-dichloro-1,3,5-triazine.**<sup>36</sup> Ammonia from a cylinder was slowly bubbled into a round-bottomed flask containing a slurry of cyanuric chloride (36.88 g, 0.2 mol) in 200 mL of dioxane and 30 mL of diglyme cooled in an ice-water bath. The temperature of the reaction was not allowed to rise above 10 °C. Addition of the gas was continued until 6.8 g (0.4 mol) had been taken up by the mixture, which took about 1 h. Nitrogen was blown through the reaction flask to remove excess NH<sub>3</sub>. The mixture was filtered, and the precipitate was washed well with THF (300 mL). The collected solutions were concentrated by rotary evaporation (first at aspirator pressure and then at 1 Torr), and the solid residue was dried under vacuum at 0.1 Torr overnight, yielding 28.34 g (0.172 mol, 86%) of a white powder, mp 228–231 °C (lit.<sup>36</sup> 235–236 °C). This material decomposed slowly in the presence of atmospheric moisture; it was stored in a desiccator. To obtain fresh aminodichlorotriazine for a

(36) This preparation is a modification of that found in: Thurston, J. T.; Dudley, J. R.; Kaiser, D. W.; Hechenbleikner, I.; Schaefer, F. C.; Holm-Hansen, D. *J. Am. Chem. Soc.* **1951**, *73*, 2981.

**Table 1.** Crystallographic Data for Cocrystals of *N,N'*-Bis(*para*-X-phenyl)melamines and 5,5-Diethylbarbituric acid (**Mel(4-X-Ph)<sub>2</sub>-Bar(Et)<sub>2</sub>**)<sup>a</sup>

X	space group	<i>a</i> (Å)	<i>b</i> (Å)	<i>c</i> (Å)	$\alpha$ (deg) <sup>b</sup>	$\beta$ (deg) <sup>b</sup>	$\gamma$ (deg) <sup>b</sup>	<i>R</i> <sup>c</sup>	$C_k^*$ <sup>d</sup>	density (g/cm <sup>3</sup> ) <sup>e</sup>	crystallization solvent
H	<i>Pnma</i>	12.940	<u>9.982</u>	17.377					0.063	0.72	1.369
F	<i>P2<sub>1</sub>/n</i>	31.627	<u>15.470</u>	<u>9.700</u>		90.08			0.044	0.69	1.395
Cl	<i>P1</i>	9.822	13.650	<u>9.228</u>	92.86	95.14	92.57	0.084	0.70	1.436	MeOH
Br (form I)	<i>P1</i>	9.826	13.742	9.389	93.67	95.11	93.30	0.061	0.71	1.636	MeOH
Br (form II)	<i>P2<sub>1</sub>/n</i>	9.735	31.396	8.417		90.47			0.044	0.68	1.602
I	<i>P2<sub>1</sub>/n</i>	8.656	31.412	9.735		90.73			0.045	0.69	1.792
CH <sub>3</sub>	<i>P2<sub>1</sub>/n</i>	9.747	8.226	<u>31.982</u>		95.46			0.093	0.68	1.276
CF <sub>3</sub>	<i>P2/n</i>	8.673	16.186	9.740		92.80			0.071	0.66	1.455

<sup>a</sup> The underlined cell dimensions represent the repeat distance in a tape, or *L* in Figure 13. <sup>b</sup> A blank means that the angle is constrained to be 90°.

<sup>c</sup> This value is the crystallographic reliability index, *R* =  $\sum|(F_0 - F_c)|/\sum F_0$ . <sup>d</sup> This value is the packing coefficient calculated using molecular volumes obtained from MacroModel<sup>31</sup> (see the Results section and footnote 34 for a discussion of the relationship between  $C_k^*$  and the "classical" packing coefficient, *C<sub>k</sub>*). <sup>e</sup> Calculated.

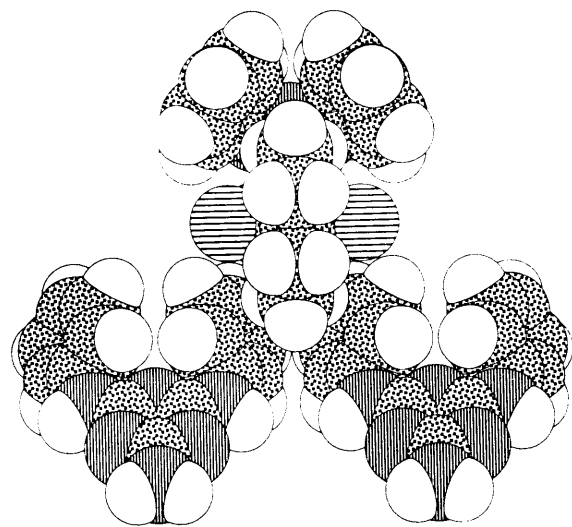


**Figure 14.** Complementary packing between phenyl and ethyl substituents in the **Mel(4-H-Ph)<sub>2</sub>-Bar(Et)<sub>2</sub>** complex. The top melamine belongs to tape B in Figure 4, the barbital to tape F, and the bottom melamines to tape G.

**Table 2.** Intratape Measurements<sup>a</sup>

	X in <b>Mel(4-X-Ph)<sub>2</sub>-Bar(Et)<sub>2</sub></b>						
	H	F <sup>b</sup>	Cl	Br <sup>c</sup>	I	CH <sub>3</sub>	CF <sub>3</sub>
intermolecular distance, <i>d</i> (Å)	4.45	3.70	3.70	3.85	4.38	4.25	4.33
		4.14		4.30			
intramolecular distance, <i>d'</i> (Å)	5.53	6.34	6.32	6.09	5.47	5.69	5.48
		5.76		5.59			
<i>d</i> + <i>d'</i> (Å)	9.98	10.04	10.02	9.94	9.85	9.94	9.81
		9.90		9.89			
van der Waals diameter of X (Å)	2.40	2.94	3.50	3.70	3.96	4.44 <sup>d</sup>	5.46 <sup>d</sup>

<sup>a</sup> See Figure 13 for depictions of parameters. <sup>b</sup> There are two melamines in the asymmetric unit of this complex. <sup>c</sup> The first and second lines give the values for the form I and form II polymorphs, respectively. <sup>d</sup> The diameters listed for CH<sub>3</sub> and CF<sub>3</sub> are calculated assuming a circular cross section for these groups. The value for CF<sub>3</sub> is therefore approximately 1.1 Å greater than *d*, but since a fluorine of one CF<sub>3</sub> group may be able to cogwheel with two fluorines on an adjacent group, steric repulsion is not necessarily as large as these diameters imply.

reaction, the stored material was stirred with dry diethyl ether (about 10 mL/g), the slurry was filtered at reduced pressure, and the solvent was removed by rotary evaporation at aspirator pressure to yield pure aminodichlorotriazine.

**General Procedure for Synthesis of 2-Amino-4,6-bis(arylamino)-1,3,5-triazines (*N,N'*-Diphenylmelamines).** **Method A.**<sup>37</sup> A 0.1 M solution of 2-amino-4,6-dichloro-1,3,5-triazine was prepared in freshly distilled THF and heated to 40–50 °C in an oil bath. To the solution in the oil bath was added a THF solution of 1 equiv of the desired aniline (0.1 M) and

(37) This preparation is a modification of that found in: Kaiser, D. W.; Thurston, J. T.; Dudley, J. R.; Schaefer, F. C.; Hechenbleikner, I.; Holm-Hansen, D. *J. Am. Chem. Soc.* **1951**, *73*, 2984.

1 equiv of diisopropylethylamine (DIEA) via a dropping funnel over the course of about 30 min with magnetic stirring. Conversion to the 2-amino-4-anilino-6-chloro-1,3,5-triazine was usually complete by the end of the addition, as shown by TLC, but heating could be continued as necessary until the reaction was complete. At that point, another equivalent of aniline was added, along with another of DIEA, in THF. The temperature of the heating bath was raised to about 100–105 °C. As the THF boiled off, 2:1 dioxane/H<sub>2</sub>O was added to keep the amount of solvent approximately constant, and a reflux condenser was attached. Reaction was usually continued for 3–5 h at 100–105 °C, but it could be prolonged as necessary, while the progress of the reaction was monitored by TLC. At completion, the reaction was cooled and poured into about 150–200 mL of H<sub>2</sub>O. The precipitated product was collected by vacuum filtration. After being dried under vacuum at 0.1 Torr, the melamine was purified by flash chromatography on silica gel.

**Method B.**<sup>37</sup> A 0.1 M solution of cyanuric chloride was prepared in freshly distilled THF and cooled in an ice–water bath. A THF solution of 1 equiv of the desired aniline (0.1 M) and 1 equiv of DIEA was added via a dropping funnel over the course of 15–30 min with magnetic stirring. When the addition was complete, the mixture was allowed to warm to room temperature, and stirring was continued for another hour. The mixture was then heated to 40–50 °C in an oil bath, and another equivalent of aniline and base was added. Heating was continued for several hours, or until TLC showed no further change. At this stage, the intermediate 2-chloro-4,6-diamino-1,3,5-triazine was usually pure enough, as determined by TLC, that it could be isolated by filtering the reaction mixture and removing solvent by rotary evaporation at aspirator pressure. The crude product was usually used directly in the next step. Flash chromatography on silica could be performed if necessary.

The 2-chloro-4,6-diamino-1,3,5-triazine (dissolved in ~5–8 mL of dioxane or THF) and a magnetic stirrer were placed in a 15-mL pressure bottle. Approximately 3–5 mL of 30% NH<sub>4</sub>OH was added, and the bottle was capped and heated (CAUTION: behind a safety shield) to 100–105 °C in an oil bath. Heating was continued for 5–8 h, after which the vial could be cooled and opened to monitor reaction progress by TLC. If an unacceptable amount of starting material remained, an additional aliquot of 30% NH<sub>4</sub>OH (2–3 mL) was added, and the vial was recapped and reheated as necessary. When reaction was judged to be complete, the solution was poured into 150–200 mL of H<sub>2</sub>O, and the precipitated product was collected by vacuum filtration. After drying under vacuum at 0.1 Torr, the crude melamine was purified by flash chromatography on silica gel.

The following summary lists the melamine (X in **Mel(4-X-Ph)<sub>2</sub>**), the method used, and the melting point of the product: H, A, 214–6 °C (lit. mp 219–20 °C<sup>37</sup>); F, B, 191–3 °C dec; Cl, B, 202–4 °C; Br, A, 243–5 °C dec; I, B, 267–70 °C dec; CH<sub>3</sub>, A, 282–4 °C dec (lit. mp 289–90 °C<sup>38</sup>); CF<sub>3</sub>, B, 218–9 °C. For spectroscopic details and elemental analyses on new compounds, see the supplementary material.

**Preparation of Complexes.** Equimolar amounts of the melamine and barbital were dissolved together (in one flask) in THF. The solvent was removed by rotary evaporation at aspirator pressure, and the composition of the complex was checked by <sup>1</sup>H NMR spectroscopy. If integration of peaks indicated that one component was present in excess, the other component was added to bring their ratio to 1:1. The melting points of the complexes were as follows: **Mel(4-H-Ph)<sub>2</sub>-Bar(Et)<sub>2</sub>**, 234–237 °C; **Mel(4-F-Ph)<sub>2</sub>-Bar(Et)<sub>2</sub>**, 238–243 °C dec; **Mel(4-Cl-Ph)<sub>2</sub>-Bar(Et)<sub>2</sub>**, 268–270 °C; **Mel(4-Br-Ph)<sub>2</sub>-Bar(Et)<sub>2</sub>** (form I), 272–275 °C dec, (form II),

(38) Honda, I. *Yuki Gosei Kagaku Kyokaishi* **1962**, *20*, 460; *Chem. Abstr.* **1963**, *58*, 4568c.

278–280 °C dec;  $\text{MeI}(4\text{-I-Ph})_2\text{-Bar(Et)}_2$ , 280–283 °C dec;  $\text{MeI}(4\text{-CH}_3\text{-Ph})_2\text{-Bar(Et)}_2$ , 270–277 °C dec;  $\text{MeI}(4\text{-CF}_3\text{-Ph})_2\text{-Bar(Et)}_2$ , 264–266 °C. The melting point of barbital is 190–192 °C.

**Crystallization of Complexes. A.  $\text{MeI}(4\text{-H-Ph})_2\text{-Bar(Et)}_2$ .** Crystals were grown by room-temperature evaporation of a solution of the complex in  $\text{CH}_2\text{Cl}_2$  in a 1-dram screw-top vial with the lid resting on top of the vial.

**B.  $\text{MeI}(4\text{-F-Ph})_2\text{-Bar(Et)}_2$ ,  $\text{MeI}(4\text{-CH}_3\text{-Ph})_2\text{-Bar(Et)}_2$ , and  $\text{MeI}(4\text{-CF}_3\text{-Ph})_2\text{-Bar(Et)}_2$ .** Crystals were grown by allowing a solution of the complex in boiling  $\text{CH}_3\text{CN}$ ,  $\text{MeOH}$ , or 2:1 pyridine/ $\text{H}_2\text{O}$ , respectively, to cool over the course of at least 24 h to room temperature by enclosing it in a corked Dewar flask.

**C.  $\text{MeI}(4\text{-Cl-Ph})_2\text{-Bar(Et)}_2$ ,  $\text{MeI}(4\text{-Br-Ph})_2\text{-Bar(Et)}_2$  (both forms), and  $\text{MeI}(4\text{-I-Ph})_2\text{-Bar(Et)}_2$ .** Crystals were grown by room-temperature evaporation of a solution of the complex in  $\text{CH}_3\text{OH}$  in a 5-mL screw-top vial with the lid resting on top of the vial.

**X-Ray Crystallography.** For details of X-ray data collection and structure solution and refinement, see the supplementary material. Data were collected on complexes  $\text{MeI}(4\text{-H-Ph})_2\text{-Bar(Et)}_2$  and  $\text{MeI}(4\text{-CH}_3\text{-Ph})_2\text{-Bar(Et)}_2$  at Harvard on a Siemens P3 diffractometer. Data on the other complexes were collected by Molecular Structure Corporation, The Woodlands, TX, on a Rigaku AFC5R diffractometer equipped with a

rotating anode generator. All structures were solved and refined at Harvard using the Siemens SHELXTL-PLUS package of programs.

**Acknowledgment.** We acknowledge the support of the National Science Foundation through Grants CHE-91-22331, to G.M.W., DMR CHE-89-20490, to the Harvard University Materials Research Laboratory, and CHE-80-00670, for the purchase of the Siemens X-ray diffractometer. J.C.M. acknowledges the Merck Corporation for financial assistance. We thank Professor Jack Dunitz for helpful comments, especially concerning polymorphism.

**Supplementary Material Available:** Techniques of crystallization, experimental details for substituted diphenylmelamines, table of hydrogen bond lengths, table of intermolecular contacts, crystallographic details including tables of atomic positional parameters and bond lengths and angles (134 pages); tables of observed and calculated structure factors (108 pages). This material is contained in many libraries on microfiche, immediately follows this article in the microfilm version of the journal, and can be ordered from the ACS; see any current masthead page for ordering information.